Imaging of the Middle and Visceral Mediastinum

Patrick P. Bourgouin, MD[a], Rachna Madan, MD[b,*]

KEYWORDS

• Visceral • Middle • Mediastinum • Lymphadenopathy • Foregut cyst • Paraganglioma

KEY POINTS

- The middle or visceral mediastinum contains the heart, great vessels, lymph nodes, the esophagus and portions of the trachea.
- Computed tomography scanning is the primary imaging modality used to identify and characterize mediastinal abnormalities. MR imaging and nuclear medicine studies can help with problem solving and refining the differential diagnosis.
- Lymphadenopathy is the most common disease process involving the visceral mediastinum and occurs with a wide variety of benign and malignant processes.
- Other abnormalities that can be diagnosed on imaging include foregut duplication cysts, neoplasms and other lesions arising from the trachea and esophagus, and paragangliomas.
- In addition to identifying, localizing, and characterizing lesions in the visceral mediastinum, imaging plays an important role in directing invasive diagnostic procedures and monitoring response to treatment.

INTRODUCTION

The middle or visceral mediastinum is notable for containing the heart, great vessels, lymph nodes, and portions of the esophagus and trachea. In terms of pathology, the most common abnormalities involving this compartment include lymphadenopathy, foregut duplication cysts such as bronchogenic and esophageal duplication cysts, tracheal and esophageal neoplasms, and other diseases. Imaging plays a key role in identifying and diagnosing these conditions as well as guiding biopsy or surgery if needed.

NORMAL ANATOMY AND IMAGING TECHNIQUE

The mediastinum contains several vascular and nonvascular structures and its division into different compartments is crucial for localization and development of an accurate differential diagnosis. The International Thymic Malignancy Interest Group has developed a classification of mediastinal compartments based on cross-sectional imaging to help with characterization of mediastinal lesions and facilitate communication among medical specialties. This classification is accepted as a standard.[1,2]

The visceral mediastinal compartment is characterized by the following boundaries: (1) the thoracic inlet superiorly, (2) the diaphragm inferiorly, (3) the anterior aspect of the pericardium anteriorly, and (4) a vertical line situated 1 cm posterior to the anterior margin of each vertebral body posteriorly. Thus, it includes several important vascular structures such as the heart, thoracic aorta, intrapericardial pulmonary arteries, superior vena cava, and thoracic duct. Nonvascular structures incorporated in this compartment include portions of the trachea, including the carina, the esophagus, and the lymph nodes.[1,2]

[a] Department of Radiology, Brigham and Women's Hospital, 75 Francis Street, Boston, MA 02115, USA; [b] Division of Thoracic Imaging, Department of Radiology, Brigham and Women's Hospital, Harvard Medical School, 75 Francis Street, Boston, MA 02115, USA
* Corresponding author.
E-mail address: rmadan@bwh.harvard.edu

Radiol Clin N Am 59 (2021) 193–204
https://doi.org/10.1016/j.rcl.2020.11.004

Anomalies of the visceral mediastinum may be initially detected on chest radiography. Although the identification of small lesions is often difficult, careful examination of the mediastinum on chest radiography may reveal unsuspected abnormalities in otherwise asymptomatic individuals. Mediastinal masses typically present with focal contour abnormalities of the mediastinum or diffuse widening of the mediastinum. Indirect signs with displacement of mediastinal lines and stripes can also be seen. In the case of a hilar or perihilar mass, the hilum overlay sign, which is defined as a visibility of the hilar vasculature through the opacity, suggests that the mass is either within the anterior or posterior compartments. A different sign, the hilum convergence sign, can help to distinguish between pulmonary artery enlargement (manifesting as pulmonary vessels that converge toward the edge of the mass-like opacity) versus a nonvascular hilar mass, such as lung malignancy or lymphadenopathy (in which vessels do not converge toward the edge of the mass-like opacity). If only a frontal radiograph is available, obtaining a lateral radiograph may be helpful in localizing mediastinal anomalies to the proper compartment. After the initial detection of a potential mediastinal lesion, further characterization with cross-sectional imaging is warranted.

Computed tomography (CT) scanning remains the imaging modality of choice to evaluate most mediastinal abnormalities owing to its widespread availability, ability to localize lesions to the correct compartment, and excellent spatial resolution. It can also be used for tissue characterization with detection of macroscopic fat, cystic components, calcification, hemorrhage, and hypervascularity.[3,4] Intravenous (IV) iodinated contrast is usually used, because it allows for an assessment of lesion enhancement and helps in differentiating potential masses from vascular structures.

MR imaging is beneficial for its excellent tissue characterization and lack of ionizing radiation.[5] Thoracic MR imaging provides greater diagnostic precision in the evaluation of indeterminate mediastinal masses on CT scan, such as complex cystic masses or masses containing intralesional fat or hemorrhage.[6,7] It can also be used as a staging study in patients with contrast allergy or renal failure, in whom a contrast-enhanced CT scan may be contraindicated.

Finally, several nuclear medicine studies may be used as additional problem-solving modalities. A PET/CT scan with fluorodeoxyglucose can be used to identify distant metastases in the setting of suspected malignancy.[8] ^{123}I-Metaiodobenzylguanidine, In-111octreotide scintigraphy, and a PET/CT scan with fluorodeoxyglucose can be used in patients with suspected paragangliomas to further narrow the differential diagnosis. 99mTc pertechnetate scans have a role in the further evaluation of suspected esophageal duplication cysts, where it can accurately localize functioning ectopic gastric mucosa.

IMAGING FINDINGS AND PATHOLOGY

Lymphadenopathy

Stations

The visceral compartment of the mediastinum includes multiple lymph node stations, including upper and lower paratracheal, subaortic, para-aortic, subcarinal, paraesophageal, and pulmonary ligamental lymph nodes.[9] The enlargement of 1 or more of these lymph nodes may be seen in a wide variety of benign and malignant processes and is the most common cause of a visceral mediastinal mass. A CT scan has greater sensitivity than chest radiography for the detection of lymph node enlargement. A PET/CT scan with fluorodeoxyglucose also plays an important role in evaluation of lymphadenopathy and in directing endobronchial ultrasound-guided biopsies.

Appearance and size

On a CT scan, lymph nodes typically appear as oval or round homogeneous masses of soft tissue attenuation in their expected anatomic location. The size criteria for abnormal lymph node enlargement have been discussed in the literature and measurements range from 10 to 15 mm depending on the location.[10,11] The sensitivity and specificity of a CT scan are limited in differentiating malignant and benign lymph node enlargement.[12] However, a CT scan can be used to guide invasive diagnostic procedures and its accessibility makes it a useful modality for monitoring treatment response.

Causes of nodal enlargement

Malignant lymphadenopathy can be seen in metastatic disease (from thoracic or extrathoracic primary neoplasms) or lymphoproliferative disorders. Benign enlargement may be seen in the context of pneumonia or pulmonary edema, an inflammatory process like sarcoidosis (**Fig. 1**), or granulomatous infection, or rarer entities like angiofollicular lymph node hyperplasia (Castleman disease, discussed in detail elsewhere in this article). The differential diagnosis can be narrowed by measuring the density of the lymph nodes and evaluating their distribution (**Tables 1** and **2**).

Lymph Node Attenuation

Hypoattenuating lymph nodes usually represent necrosis and are commonly seen in metastatic disease (**Fig. 2**) or atypical infectious processes

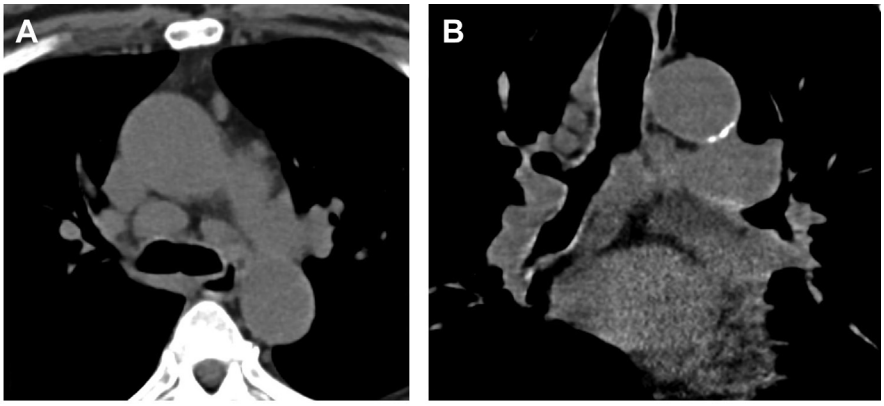

Fig. 1. Sarcoidosis. Axial (*A*) and coronal (*B*) images from an unenhanced CT scan of the chest demonstrates mild enlargement of multiple lymph nodes in the visceral compartment (paratracheal and subcarinal stations).

caused by fungal or mycobacterial agents.[13,14] Much rarer entities include sprue and necrotizing lymphadenitis (Kikuchi–Fujimoto disease).[15]

A hyperattenuating appearance of the lymph nodes may be due to the presence of calcification or mineral dust or due to hypervascularity. The presence of calcifications or other dense inorganic materials can be seen in sarcoidosis, remote granulomatous infection (most commonly tuberculosis and histoplasmosis), treated lymphoproliferative disorders, amyloidosis, and pneumoconioses, such as silicosis and berylliosis.[16] Metastases from thyroid carcinoma and mucinous adenocarcinoma may also calcify.

Hypervascular lymphadenopathy, characterized by brisk enhancement after IV contrast administration, can be seen in metastatic disease, usually from a select group of tumors, including renal cell carcinoma, melanoma, papillary thyroid carcinoma, sarcoma, and neuroendocrine tumors (**Box 1**, **Table 3**). Rarer entities include angiofollicular lymph node hyperplasia (Castleman disease) and Kaposi sarcoma.[17,18] Kikuchi–Fujimoto and Kimura diseases, commonly presenting with cervical lymphadenopathy, can also cause mediastinal lymph node enlargement.[15,19]

Table 1
Differential diagnosis for multistation lymphadenopathy

Category	Possible Causes
Neoplastic	Metastases, lymphoproliferative disorders
Infectious	Mycobacterial and fungal infection
Inflammatory	Sarcoidosis
Pneumoconioses	Silicosis, coal worker's pneumoconiosis, berylliosis
Reactive	Pulmonary edema, interstitial lung disease

Patterns of Lymph Node Enlargement in Neoplastic and Non-neoplastic Entities

An understanding of lymphatic drainage pathways is helpful in directing attention to relevant stations when interpreting an imaging examination, especially for the staging of cancer. The distribution of lymphadenopathy can also give clues as to the site of the primary tumor in the setting of metastatic disease or suggest alternative diagnoses.

Table 2
Differential diagnosis for causes of lymphadenopathy based on CT appearance

Lymph Node Density	Possible Causes
Hypoattenuating	Cystic or necrotic metastases, mycobacterial and fungal infections, lymphoma
Hyperattenuating	Sarcoidosis, silicosis and other pneumoconiosis (berylliosis), prior granulomatous infection, amyloidosis, treated lymphoma
Hyperenhancing	Hypervascular metastases, Castleman disease, Kaposi sarcoma

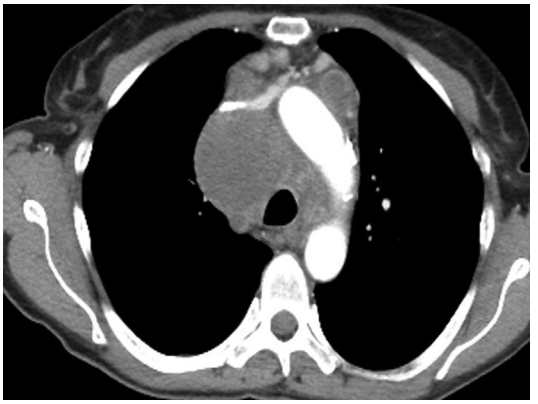

Fig. 2. Metastatic lung cancer. A contrast-enhanced axial CT scan of the chest of a patient with lung cancer shows multiple enlarged nodes in the visceral compartment (right paratracheal station) and prevascular mediastinum with central low attenuation and peripheral rim enhancement indicating extensive necrosis. Note the mass effect exerted on adjacent mediastinal structures.

Lung neoplasms usually drain first to the hilar lymph nodes, although direct mediastinal involvement is also possible. Subsequent drainage pathways in the mediastinum depend on the lobe of origin. Right upper lobe tumors drain into the right paratracheal and anterior mediastinal lymph nodes, whereas lesions of the middle and lower lobes drain into the subcarinal lymph nodes before continuing to the right paratracheal lymph nodes. Left upper lobe tumors drain preferentially to the para-aortic and subaortic lymph nodes, whereas those in the left lower lobe favor the subcarinal and subaortic stations.[20]

The upper two-thirds of the esophagus generally drain cranially, whereas the lower one-third drains caudally. Therefore, neoplasia involving the upper two-thirds tend to involve the paratracheal lymph nodes, whereas tumors of the lower one-third preferentially involve the gastrohepatic lymph nodes. The esophageal lymphatics communicate with the thoracic duct; distant nodal metastases are also possible.[21]

Box 1
Importance of detecting hypervascularity within a visceral mediastinal mass

Narrows differential diagnosis to a small group of entities.

Entails propensity to bleed and need for careful preprocedure planning, including embolization before any procedure.

Percutaneous biopsy may not be safe; surgical biopsy allowing for better control of hemorrhage may be preferred.

Enlargement of the lymph nodes involving multiple mediastinal stations and bilateral hila can be seen in lymphoproliferative disorders. Hodgkin lymphoma in particular involves the mediastinum in up to 85% of cases, especially the superior paratracheal stations and prevascular mediastinum. Non-Hodgkin lymphoma may also involve the mediastinum but does so less frequently and sometimes present as lymphadenopathy in a single station.

Sarcoidosis is a common cause of bilateral hilar lymph node enlargement and should be a leading differential in the absence of known malignancy. Involvement of the paratracheal and subcarinal lymph nodes is also frequent.[22] Pneumoconioses such as silicosis and coal worker's disease can also manifest with a similar distribution, as well as fungal and mycobacterial infections. As outlined elsewhere in this article, measuring the internal density of these lymph nodes may help to narrow the differential diagnosis. Finally, mild diffuse lymph node enlargement can also be seen in reaction to diffuse lung processes, such as pulmonary edema and interstitial lung disease.

Castleman Disease

Angiofollicular lymph node hyperplasia, also known as Castleman disease (**Fig. 3**), is a rare benign lymphoproliferative disease that frequently presents as a mediastinal mass. Although it can also affect the cervical and abdominal lymph nodes, approximately 70% occur in the chest, and the visceral mediastinum is the most common location.[17,23,24]

Castleman disease has been historically subdivided based on unicentric or multicentric involvement of lymph nodes. However, the modern histopathologic classification recognizes 4 main entities: hyaline vascular Castleman disease, plasma cell Castleman disease, human herpes virus-8–associated Castleman disease, and Castleman disease not otherwise specified. The imaging appearance is typically that of hyperenhancing lymph node enlargement involving 1 or multiple stations. Histologic confirmation is usually necessary for a diagnosis. The differential diagnosis depends on the compartments involved and associated imaging findings. For example, unicentric disease may mimic thymoma, sarcoma, and paraganglioma, whereas multicentric disease resembles lymphoma, metastatic disease, and sarcoidosis, among other diseases.

Table 3
Differential diagnosis for hypervascular mediastinal masses

Benign	Malignant or Malignant Potential	Metastases
Castleman's disease	Sarcomas	Renal cell carcinoma
Ectopic parathyroid adenoma	Paraganglioma	Thyroid carcinoma
Vascular malformations	Carcinoid	Melanoma
	Castleman's disease	Pheochromocytoma
		Carcinoid
		Choriocarcinoma

The hyaline vascular variant comprises 90% of cases and most commonly manifests as unicentric disease, presenting as a solitary hyperenhancing mass in a young adult. The differential diagnosis depends on the affected mediastinal compartment and includes thymoma, lymphoma, sarcoma, and neurogenic tumors. In the absence of IV contrast, complicated foregut duplication cysts may have a similar appearance.

The plasma cell variant most commonly presents as multicentric disease and tends to involve older adults. Lymph node enlargement involving multiple mediastinal compartments and bilateral hila is seen although enhancement following IV contrast administration is reportedly less than that for the hyaline variant. The main differential diagnosis is lymphoma and other causes of multistation lymphadenopathy, such as sarcoidosis and metastatic disease. Systemic manifestations such as fever, night sweats, and anemia are more common, and the entity has been linked to lymphocytic interstitial pneumonitis.[25]

Human herpes virus-8–associated Castleman disease has a poor prognosis and typically affects immunocompromised patients. It commonly presents as multicentric disease with severe systemic manifestations. The imaging appearance is similar to an aggressive form of plasma cell Castleman disease.

Trachea

Bronchogenic cyst Bronchogenic cysts are congenital foregut malformations typically presenting as well-circumscribed masses with homogeneous internal fluid attenuation and thin or imperceptible wall.[26] Up to 90% are in the visceral mediastinum, usually close to the carina or in the right paratracheal space, although intrapulmonary cysts are also possible.[27] The internal density is usually that of fluid, but variable proteinaceous, mucoid, or hemorrhagic content may increase attenuation, making the distinction between a cyst and a soft tissue mass difficult.[28] After IV contrast administration, the wall may enhance, but there should be no enhancing component within the mass. Because it is easy to misinterpret hyperattenuating cystic lesions as solid on both noncontrast and contrast-enhanced CT scans,

Fig. 3. Castleman disease. (*A*) An unenhanced axial CT scan of the chest demonstrates a large solid lobulated visceral mediastinal mass with branching calcifications. (*B*) A contrast-enhanced coronal reformation from a CT scan of the chest shows brisk heterogeneous enhancement with numerous feeding vessels in the periphery of the mass in keeping with the hypervascular nature of the lesion.

the use of MR imaging is critical to make this distinction and prevent unnecessary follow-up and diagnostic interventions. When a mediastinal mass is well-circumscribed, homogeneous in attenuation, and round or oval in configuration, MR imaging should be considered to distinguish between a cystic and a solid lesion.[29] On T2-weighed images, a bronchogenic cyst should have high signal intensity. The T1 signal can be variably high, depending on proteinaceous or hemorrhagic content[30,31] (**Fig. 4**).

Bronchogenic cysts should not normally communicate with the bronchial tree and the presence of internal gas may signify a superimposed infection.[32] They may cause symptoms such as cough or recurrent pneumonia through compression of adjacent structures such as the airway. Malignant transformation is possible, but very rare.

The differential diagnosis includes other congenital cystic lesions of the mediastinum, such as esophageal duplication cysts, pericardial cysts, and cystic neurogenic lesions. Abscesses, hematomas, and seromas should be considered in the appropriate clinical setting. Lymphatic malformations can be seen typically in pediatric patients. Finally, neoplasia with cystic components should be considered, particularly when enhancing internal components are seen.

Tracheal tumors and tumor-like entities Tracheal neoplasms can be seen on CT scans as a focal thickening of the tracheal wall or nodular lesions that extend into the lumen. The differentiation of benign and malignant lesions is often not possible on imaging alone, unless the lesion is large and results in the invasion of adjacent mediastinal structures. CT scans and virtual bronchoscopy can be used to direct endoscopy for biopsy and definitive diagnosis.[33,34]

Primary malignant neoplasms include squamous cell carcinoma, which is strongly associated with smoking and typically occurs in the distal one-third of the trachea, and adenoid cystic carcinoma (**Fig. 5**), which is not associated with smoking and usually occurs in the distal trachea and proximal bronchi. Mucoepidermoid carcinoma is typically encountered in young adults and presents as a nodule in the main bronchi or, less commonly, in the trachea. Benign lesions include carcinoid, papilloma, hamartoma, and chondroma.[35] Carcinoid tumors typically present as enhancing endobronchial nodules that may calcify. Tracheal papillomatosis occurs after human papilloma virus infection, either from colonization during birth or rarely from dissemination from laryngeal papillomatosis. A CT scan will demonstrate numerous small nodules in the airways and cavitating lung nodules. Finally,

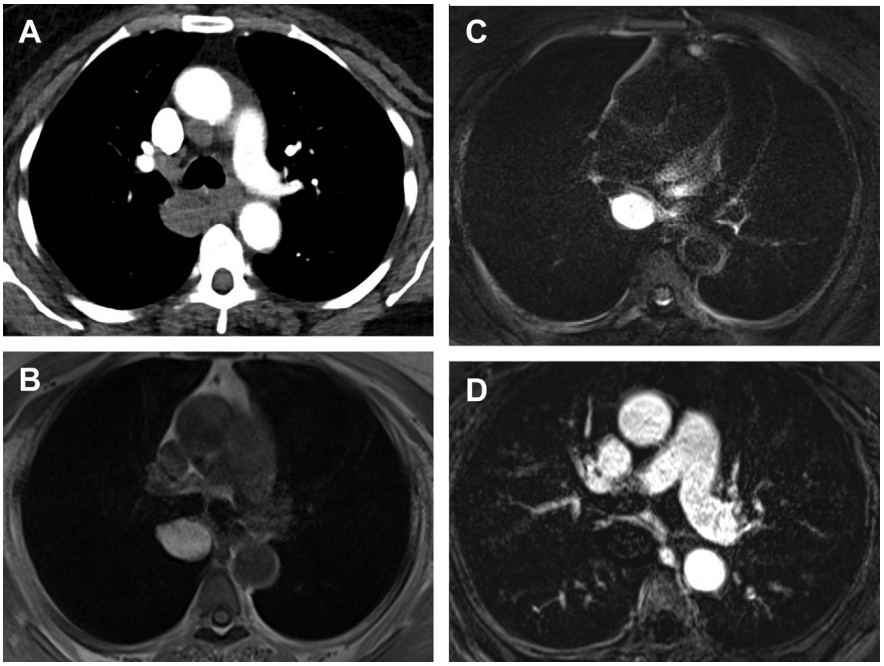

Fig. 4. Bronchogenic cyst. (*A*) A contrast-enhanced axial CT scan of the chest shows a round, well-circumscribed, homogeneous, and fluid-attenuating mass in the subcarinal region. Axial T1-weighted (*B*), axial fat-suppressed T2-weighted (*C*), and axial post-contrast T1-weighted (*D*) MR images show a heterogeneous T1 hyperintense and homogeneous T2 hyperintense mass without internal nodularity or septation that does not enhance following the administration of IV gadolinium contrast..

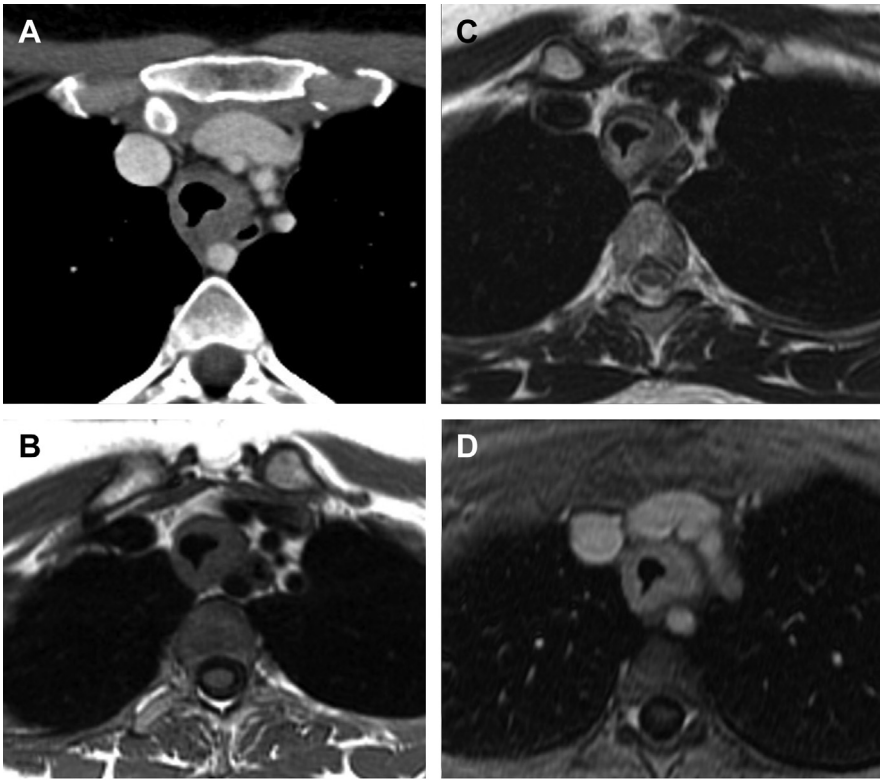

Fig. 5. Adenoid cystic carcinoma. (*A*) A contrast-enhanced axial CT image of the chest demonstrates smooth, circumferential and asymmetric thickening of the tracheal wall. Axial T1-weighted (*B*), axial T2-weighted (*C*), and axial post-contrast T1-weighted (*D*) images better demonstrate mural stratification and enhancing tumor.

it is important to consider foreign bodies, especially in pediatric patients.

Non-neoplastic tracheal disorders Tracheal strictures can be seen on a CT scan as focal areas of narrowing. They can occur after prolonged endotracheal intubation or from prior infection, surgery, or inhalation injury.[33]

Diffuse tracheal narrowing is seen in tracheomalacia, causing excessive airway collapse during expiration. The diagnosis can be made on a CT scan when there is a 50% or greater decrease in the transverse tracheal diameter during expiration.[36] This entity is to be distinguished from saber-sheath trachea, which is usually seen in chronic obstructive pulmonary disease and is defined as a coronal diameter that is two-thirds of the sagittal diameter.[37]

Tracheobronchomegaly, also known as Mounier–Kuhn syndrome, is a very rare congenital disorder causing diffuse dilatation of the trachea and central bronchi. Affected patients typically present with recurrent infections.[38]

Thickening of the tracheal wall can be seen in a variety of inflammatory conditions (**Table 4**). Relapsing polychondritis causes diffuse smooth thickening that usually spares the posterior wall.[39] In contrast, granulomatosis with polyangiitis can cause circumferential thickening, though airway involvement is uncommon.[40] Tracheopathia osteochondroplastica is a rare disease causing multiple osteocartilaginous nodules in the tracheal submucosa, typically seen as multiple small calcifying nodules sparing the posterior wall. Amyloidosis can have a similar appearance, although the posterior wall is not spared.[35]

Esophagus

Esophageal duplication cyst Esophageal duplication cysts are rare congenital foregut malformations presenting as well-circumscribed masses near the esophagus or associated with the esophageal wall. They are typically of homogeneous fluid attenuation, although a greater density can be seen with hemorrhage or infection. These complications can be seen particularly when the cyst contains ectopic gastric mucosa, the presence of which makes 99mTc pertechnetate scans helpful in narrowing down the differential diagnosis.[41] As with other congenital cysts, there should be no internal enhancement with IV contrast. On MR imaging, high T2 signal and variable T1 signal

Table 4
Differential diagnosis for tracheal tumors and tumor-like entities

Pattern of Involvement	Possible Causes
Focal	Malignant: squamous cell carcinoma, adenoid cystic carcinoma, mucoepidermoid carcinoma Benign: carcinoid, hamartoma, foreign body
Diffuse	Posterior wall sparing: Relapsing polychondritis, tracheopathia osteochondroplastica Circumferential: Amyloidosis, sarcoidosis, granulomatosis with polyangiitis, papillomatosis

(depending on the degree of hemorrhagic or proteinaceous content) are typical.

Esophageal duplication cysts may cause symptoms from the compression of adjacent structures, including dysphagia and pain.[32] Airway obstruction is also possible, especially in infants with cysts located superiorly to the carina.[42]

As described elsewhere in this article, the differential diagnosis includes other congenital cystic lesions, abscesses, hematomas, seromas, and cystic neoplasms.

Other esophageal lesions The esophagus should be carefully assessed for masses or wall thickening. Circumferential wall thickening can be seen in esophagitis, either from infectious or inflammatory causes, or neoplasia. Asymmetric or nodular thickening raises concern for malignancy, usually squamous cell carcinoma (**Fig. 6**) or adenocarcinoma.[1] Lesions of the distal one-third of the esophagus are more likely to represent adenocarcinoma because of the association with esophageal reflux. The identification of such lesions warrants investigation with endoscopy and possible biopsy for a definitive diagnosis.

Benign lesions, such as papillomas and lipomas, are usually difficult to diagnose on imaging alone because of their small size. Hiatus hernias may mimic a mediastinal mass on chest radiography, although a CT scan is usually diagnostic. Esophageal varices, often seen in the setting of cirrhosis and portal hypertension, manifest as serpiginous vascular structures.

Neurogenic tumors

Paragangliomas (extra-adrenal pheochromocytomas) arise from chromaffin cells, which are present in the para-aortic ganglia and can therefore present as visceral mediastinal masses, most commonly along the lesser curvature of the aorta.[43] Mediastinal paragangliomas are typically nonsecretory, but those located in the lower mediastinum can be secretory and can lead to catecholamine excess.[44]

Paragangliomas tend to be highly vascular tumors and therefore present on CT scans as briskly enhancing masses (**Fig. 7**). Areas of internal hypoenhancement may be seen and correlate with necrosis. On MR imaging, the lesions typically show intermediate signal on T1-weighted images and hyperintensity on T2-weighted images (the so-called light bulb sign). Foci of hypointensity corresponding with flow voids may also be seen with a resultant salt and pepper appearance.[45] ^{123}I-metaiodobenzylguanidine can also be helpful in narrowing the differential. Malignant paragangliomas can be seen to invade nearby structures and cause metastasis.[46]

Paragangliomas are associated with succinate dehydrogenase mutations. In particular, mutations of subunit B (SDHB) can lead to metastatic disease in more than 40% of patients.[47] MR imaging is favored to monitor patients with known SDHB mutation owing to the lack of associated ionizing radiation.

Mesenchymal lesions

Lesions of adipose tissue Mediastinal lipomatosis and lipomas are benign entities that can be diagnosed on imaging. Lipomatosis refers to increased fat in the mediastinum without a surrounding capsule, whereas a lipoma is an encapsulated and well-circumscribed fat-containing mass. In both cases, the fat content should be homogeneous and follow subcutaneous fat density on CT scans and signal on MR imaging.[48]

Mediastinal liposarcomas are malignant tumors that can rarely arise in the visceral mediastinum (**Fig. 8**). They tend to appear heterogeneous with internal soft tissue densities on CT scan. MR imaging is particularly useful at demonstrating intralesional fat, appearing hyperintense on T1- and T2-weighted images and hypointense on saturated sequences, with interspersed enhancing soft tissue. A mass effect and invasion of adjacent structures can also be seen.[49,50]

Other mesenchymal tumors Hemangiomas are benign vascular neoplasms, whereas vascular malformations represent a wide variety of nonneoplastic vascular lesions. These entities are

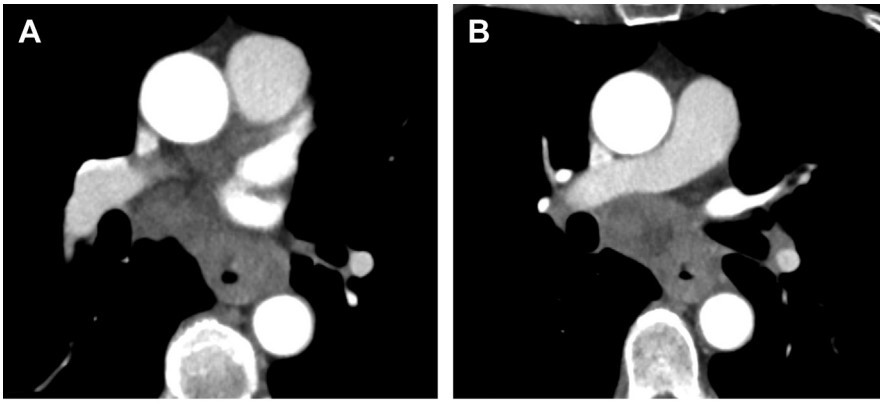

Fig. 6. Squamous cell carcinoma of the esophagus. Axial images from a contrast-enhanced chest CT demonstrating asymmetric thickening of the esophageal wall (*A*) and necrotic subcarinal lymphadenopathy (*B*).

very rare in the visceral mediastinum. Hemangiomas present as enhancing masses, whereas vascular malformations have a wide range of appearance depending on the involved vessels and lymphatics. Other rare entities include mediastinal fibromatosis, solitary fibrous tumors, inflammatory myofibroblastic tumor and sarcomas.

Mediastinitis

Mediastinitis (**Fig. 9**) involving the visceral mediastinum can be seen after traumatic or iatrogenic damage to the esophagus or airway.[51] It may also be seen as a complication of cardiothoracic surgery. The spread of infection from adjacent compartments, particularly from the neck into the superior mediastinum, may also extend into the visceral mediastinum.

Although mediastinitis and abscesses can be suggested by mediastinal widening on chest radiography, CT scanning is the imaging modality of choice and demonstrates diffuse fat stranding. A fluid collection with enhancing walls and gas content is suggestive of an abscess.[51] Air bubbles may suggest airway or esophageal perforation, and these structures must then be carefully assessed to identify the potential origin of the leak. Using water-soluble oral contrast is useful in localizing an esophageal leak and can be used to direct endoscopy procedures.[52] The differential diagnosis includes postoperative edema or hemorrhage, either from surgery or trauma.

Other complex cystic lesions

Cystic mediastinal masses include a wide range of congenital, developmental, infectious, inflammatory, and neoplastic processes. Although some cystic masses can be definitively diagnosed on CT scans, others remain indeterminate. Because of its intrinsic superior soft tissue resolution, MR imaging is an important tool in the evaluation of select mediastinal masses that are incompletely characterized on CT scanning. Besides complex bronchopulmonary foregut duplication cysts, cystic lymphangiomas and tumors with cystic degeneration described elsewhere in this article, miscellaneous entities such as postoperative

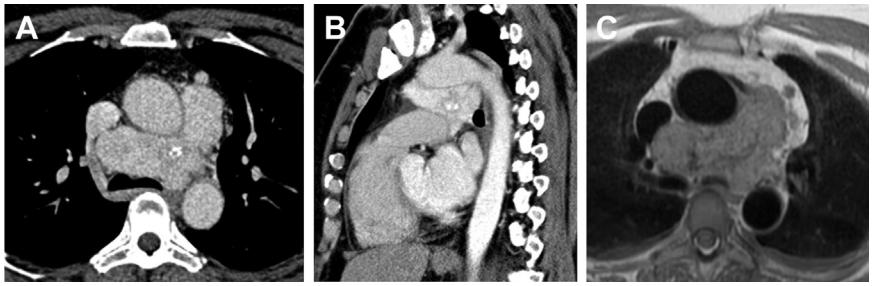

Fig. 7. Paraganglioma. A contrast-enhanced axial (*A*) and sagittal (*B*) CT scan of the chest demonstrates an avidly enhancing mass in the aortopulmonary window in close proximity to the inferior aspect of the aortic arch and superior aspect of the pulmonary arteries. The mass contains several calcifications. (*C*) Black blood double inversion recovery (DIR) axial MR image shows the invasive nature of the mass.

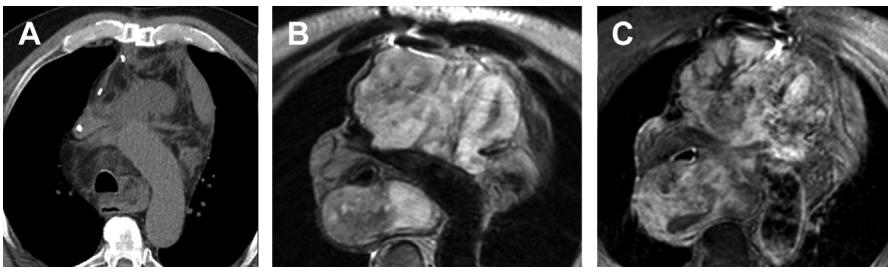

Fig. 8. Liposarcoma. (*A*) An unenhanced axial CT scan of the chest shows an infiltrative mass involving multiple compartments, including the visceral mediastinum, with regions of fat and soft tissue attenuation. (*B*) Axial T2-weighted MR image demonstrates internal foci of high signal intensity corresponding to fat. (*C*) Axial postcontrast T1-weighed MR image shows heterogeneous enhancement throughout the lesion.

hematomas and seromas and pancreatic pseudocysts can also present as cystic lesions within the visceral compartment. Occasionally, a high riding superior aortic recess of the pericardium may also mimic a cystic lesion or necrotic adenopathy in the right paratracheal region.

Lesions originating from other mediastinal compartments

Although dividing the mediastinum in compartments is helpful in establishing a differential diagnosis, it is important to keep in mind that lesions may transgress a given compartment. In the setting of a very large mass, identifying its point of origin may prove to be difficult. Thus, lesions originating in either the prevascular or paravertebral mediastinum must be kept in mind when faced with a visceral mediastinal mass. Additionally, lung masses may also invade the visceral mediastinum.

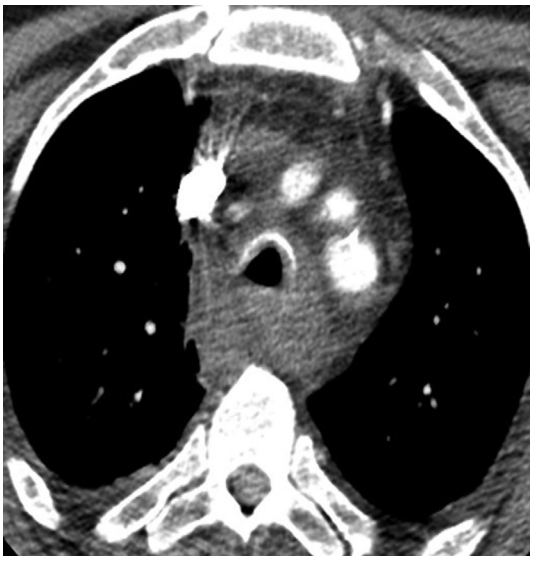

Fig. 9. Mediastinitis. A contrast-enhanced axial CT scan of the chest demonstrates diffuse infiltration of the mediastinal fat surrounding the trachea and esophagus in this patient with dysphagia and fevers, consistent with the diagnosis of mediastinitis. Endoscopy did not identify esophageal perforation. The patient was treated empirically with antibiotics and the findings resolved on subsequent imaging.

SUMMARY

Accurate identification and characterization of a mass in the visceral mediastinum usually allows for the development of a focused differential diagnosis. Although lymphadenopathy is the most common process, a select group of other identities can often be diagnosed on imaging by using a variety of modalities. Imaging also plays a key role in guiding invasive diagnostic procedures and monitoring treatment response.

CLINICS CARE POINTS

- The middle or visceral mediastinum is located between the thoracic inlet and the diaphragm in the craniocaudal axis and between the anterior aspect of the pericardium and a vertical line situated 1 cm posteriorly to the anterior margin of the vertebral bodies in the anteroposterior axis.
- Chest radiography, CT scans, MR imaging, and nuclear medicine studies can be used to detect, characterize, and diagnose abnormalities in this compartment. Imaging also plays an important role in directing invasive diagnostic procedures and monitoring the treatment response.

- Lymphadenopathy is the most common disease process involving the visceral mediastinum. Common malignant causes include metastases and lymphoproliferative disorders. Benign causes include infection (particularly from mycobacterial and fungal agents), sarcoidosis, and pneumoconioses.
- Foregut malformations such as bronchogenic cysts and esophageal duplication cysts are rare entities that may present as homogeneous cystic masses with no internal enhancement. In many cases, they can be reliably diagnosed on imaging alone. Potential pitfalls include increased attenuation from hemorrhagic or proteinaceous content and wall enhancement, which may prompt further evaluation with MR imaging.
- Paragangliomas, which can be nonsecretory or secretory and lead to catecholamine excess, may occur in the visceral mediastinum and manifest as avidly enhancing masses in close proximity to the great vessels.
- Neoplasms of the trachea and esophagus may be difficult to identify because of their small size and differentiation between malignant and benign entities is often not possible on imaging alone. The main role of imaging is to detect these anomalies, direct endoscopy, and monitor treatment response.
- Mediastinitis, with or without abscess, may occur after esophageal or airway perforation, cardiothoracic surgery, or trauma. A CT scan can be used to investigate for possible complications.

DISCLOSURE

The authors have nothing to disclose.

REFERENCES

1. Carter BW, Benveniste MF, Madan R, et al. ITMIG classification of mediastinal compartments and multidisciplinary approach to mediastinal masses. Radiographics 2017;37(2):413–36.
2. Carter BW, Tomiyama N, Bhora FY, et al. A modern definition of mediastinal compartments. J Thorac Oncol 2014;9(9 Suppl 2):S97–101.
3. Reiser M. Multidetector-row CT of the Thorax. Springer-Verlag Berlin Heidelberg: Springer Science & Business Media; 2004.
4. Rydberg J, Buckwalter KA, Caldemeyer KS, et al. Multisection CT: scanning techniques and clinical applications. Radiographics 2000;20(6):1787–806.
5. Broncano J, Alvarado-Benavides AM, Bhalla S, et al. Role of advanced magnetic resonance imaging in the assessment of malignancies of the mediastinum. World J Radiol 2019;11(3):27–45.
6. Ackman JB. MR imaging of mediastinal masses. Magn Reson Imaging Clin N Am 2015;23(2):141–64.
7. Carter BW, Betancourt SL, Benveniste MF. MR imaging of mediastinal masses. Top Magn Reson Imaging 2017;26(4):153–65.
8. Kubota K, Yamada S, Kondo T, et al. PET imaging of primary mediastinal tumours. Br J Cancer 1996; 73(7):882–6.
9. El-Sherief AH, Lau CT, Wu CC, et al. International association for the study of lung cancer (IASLC) lymph node map: radiologic review with CT illustration. Radiographics 2014;34(6):1680–91.
10. Staples CA, Müller NL, Miller RR, et al. Mediastinal nodes in bronchogenic carcinoma: comparison between CT and mediastinoscopy. Radiology 1988; 167(2):367–72.
11. McLoud TC, Bourgouin PM, Greenberg RW, et al. Bronchogenic carcinoma: analysis of staging in the mediastinum with CT by correlative lymph node mapping and sampling. Radiology 1992;182(2): 319–23.
12. Prenzel KL, Mönig SP, Sinning JM, et al. Lymph node size and metastatic infiltration in non-small cell lung cancer. Chest 2003;123(2):463–7.
13. Suwatanapongched T, Gierada DS. CT of thoracic lymph nodes. Part II: diseases and pitfalls. Br J Radiol 2006;79(948):999–1000.
14. Im JG, Song KS, Kang HS, et al. Mediastinal tuberculous lymphadenitis: CT manifestations. Radiology 1987;164(1):115–9.
15. Błasiak P, Jeleń M, Rzechonek A, et al. Histiocytic necrotising lymphadenitis in mediastinum mimicking thymoma or lymphoma - case presentation and literature review of Kikuchi Fujimoto disease. Polish J Pathol 2016;67(1):91–5 [quiz: 96].
16. Gross BH, Schneider HJ, Proto AV. Eggshell calcification of lymph nodes: an update. AJR Am J Roentgenol 1980;135(6):1265–8.
17. McAdams HP, Rosado-de-Christenson M, Fishback NF, et al. Castleman disease of the thorax: radiologic features with clinical and histopathologic correlation. Radiology 1998;209(1):221–8.
18. Herts BR, Megibow AJ, Birnbaum BA, et al. High-attenuation lymphadenopathy in AIDS patients: significance of findings at CT. Radiology 1992;185(3): 777–81.
19. Kumar V, Mittal N, Huang Y, et al. A case series of Kimura's disease: a diagnostic challenge. Ther Adv Hematol 2018;9(7):207–11.
20. Sharma A, Fidias P, Hayman LA, et al. Patterns of lymphadenopathy in thoracic malignancies. Radiographics 2004;24(2):419–34.
21. Riquet M, Saab M, Le Pimpec Barthes F, et al. Lymphatic drainage of the esophagus in the adult. Surg Radiol Anat 1993;15(3):209–11.

22. Criado E, Sánchez M, Ramírez J, et al. Pulmonary sarcoidosis: typical and atypical manifestations at high-resolution CT with pathologic correlation. Radiographics 2010;30(6):1567–86.
23. Bonekamp D, Horton KM, Hruban RH, et al. Castleman disease: the great mimic. Radiographics 2011; 31(6):1793–807.
24. Kligerman SJ, Auerbach A, Franks TJ, et al. Castleman disease of the thorax: clinical, radiologic, and pathologic correlation: from the radiologic pathology archives. Radiographics 2016;36(5):1309–32.
25. Johkoh T, Müller NL, Ichikado K, et al. Intrathoracic multicentric Castleman disease: CT findings in 12 patients. Radiology 1998;209(2):477–81.
26. McAdams HP, Kirejczyk WM, Rosado-de-Christenson ML, et al. Bronchogenic cyst: imaging features with clinical and histopathologic correlation. Radiology 2000;217(2):441–6.
27. Zylak CJ, Eyler WR, Spizarny DL, et al. Developmental lung anomalies in the adult: radiologic-pathologic correlation. Radiographics 2002;22 Spec No:S25–43.
28. Mendelson DS, Rose JS, Efremidis SC, et al. Bronchogenic cysts with high CT numbers. AJR Am J Roentgenol 1983;140(3):463–5.
29. Murayama S, Murakami J, Watanabe H, et al. Signal intensity characteristics of mediastinal cystic masses on T1-weighted MRI. J Comput Assist Tomogr 1995;19(2):188–91.
30. Nakata H, Egashira K, Watanabe H, et al. MRI of bronchogenic cysts. J Comput Assist Tomogr 1993;17(2):267–70.
31. Odev K, Arıbaş BK, Nayman A, et al. Imaging of cystic and cyst-like lesions of the mediastinum with pathologic correlation. J Clin Imaging Sci 2012;2:33.
32. Jeung MY, Gasser B, Gangi A, et al. Imaging of cystic masses of the mediastinum. Radiographics 2002;22 Spec No:S79–93.
33. Miller WT Jr. Obstructive diseases of the trachea. Semin Roentgenol 2001;36(1):21–40.
34. Finkelstein SE, Schrump DS, Nguyen DM, et al. Comparative evaluation of super high-resolution CT scan and virtual bronchoscopy for the detection of tracheobronchial malignancies. Chest 2003;124(5): 1834–40.
35. Shepard JO, Flores EJ, Abbott GF. Imaging of the trachea. Ann Cardiothorac Surg 2018;7(2):197–209.
36. Baroni RH, Feller-Kopman D, Nishino M, et al. Tracheobronchomalacia: comparison between end-expiratory and dynamic expiratory CT for evaluation of central airway collapse. Radiology 2005;235(2): 635–41.
37. Ciccarese F, Poerio A, Stagni S, et al. Saber-sheath trachea as a marker of severe airflow obstruction in chronic obstructive pulmonary disease. Radiol Med 2014;119(2):90–6.
38. Shin MS, Jackson RM, Ho KJ. Tracheobronchomegaly (Mounier-Kuhn syndrome): CT diagnosis. AJR Am J Roentgenol 1988;150(4):777–9.
39. Lee KS, Ernst A, Trentham DE, et al. Relapsing polychondritis: prevalence of expiratory CT airway abnormalities. Radiology 2006;240(2):565–73.
40. Stein MG, Gamsu G, Webb WR, et al. Computed tomography of diffuse tracheal stenosis in Wegener granulomatosis. J Comput Assist Tomogr 1986; 10(5):868–70.
41. Ferguson CC, Young LN, Sutherland JB, et al. Intrathoracic gastrogenic cyst–preoperative diagnosis by technetium pertechnetate scan. J Pediatr Surg 1973;8(5):827–8.
42. Macpherson RI. Gastrointestinal tract duplications: clinical, pathologic, etiologic, and radiologic considerations. Radiographics 1993;13(5):1063–80.
43. Buchanan SN, Radecki KM, Chambers LW. Mediastinal paraganglioma. Ann Thorac Surg 2017;103(5): e413–4.
44. Else T, Greenberg S, Fishbein L. Hereditary paraganglioma-pheochromocytoma syndromes. In: Adam MP, Ardinger HH, Pagon RA, et al, editors. GeneReviews(®). Seattle (WA): University of Washington, Seattle; 1993. p. 6. Copyright © 1993-2020, University of Washington, Seattle. GeneReviews is a registered trademark of the University of Washington, Seattle. All rights reserved.
45. Olsen WL, Dillon WP, Kelly WM, et al. MR imaging of paragangliomas. AJR Am J Roentgenol 1987; 148(1):201–4.
46. Wald O, Shapira OM, Murar A, et al. Paraganglioma of the mediastinum: challenges in diagnosis and surgical management. J Cardiothorac Surg 2010;5: 19.
47. Lenders JW, Duh QY, Eisenhofer G, et al. Pheochromocytoma and paraganglioma: an endocrine society clinical practice guideline. J Clin Endocrinol Metab 2014;99(6):1915–42.
48. Boiselle PM, Rosado-de-Christenson ML. Fat attenuation lesions of the mediastinum. J Comput Assist Tomogr 2001;25(6):881–9.
49. Miura K, Hamanaka K, Matsuoka S. Primary mediastinal dedifferentiated liposarcoma: five case reports and a review. Thorac Cancer 2018;9(12):1733–40.
50. Stark P, Eber CD, Jacobson F. Primary intrathoracic malignant mesenchymal tumors: pictorial essay. J Thorac Imaging 1994;9(3):148–55.
51. Carrol CL, Jeffrey RB Jr, Federle MP, et al. CT evaluation of mediastinal infections. J Comput Assist Tomogr 1987;11(3):449–54.
52. Madan R, Laur O, Crudup B, et al. Imaging of iatrogenic oesophageal injuries using optimized CT oesophageal leak protocol: pearls and pitfalls. Br J Radiol 2018;91(1083):20170629.